Contents

Chapter 1

Scanning over the Parameters of the Design Simulation

This section presents the results of scanning over the parameters of the PL38 and the FID38 design electrostatic simulation. These scan aims at understanding the influence of each parameter on the ionization channel operation. All the design parameters were introduced in the previous chapter **??**. For a prompt description of the parameters of the PL38 design, the reader should refer to the table **??** and the scheme **??**. For parameters relative to the FID38 design, the reader should refer to the table **??** and the scheme **??**. This chapter first introduces the methodology used for the parametric scan. It follows with a study of the impact of design parameters shared by both the PL38 and the FID38 design. Then are presented the studies on the influence of parameters specific to the PL38 design and the FID38 design.

1.1 Parametric Scanning Methodology

As discussed in the previous chapter **??**, the performances of the ionization channel mainly hold in a good charge collection and the a low baseline resolution. In order to have a low baseline resolution, the ionization channel should present a low level of noise and the high signal sensitivity. In the paragraph **??**, the resolution is deduced from the computation of the signal sensitivity and the noise level of the two detectors designs. These computation are based on the Maxwell matrix capacitance obtained from the electrostatic simulation of PL38 and FID38 designs. Scanning the multi-dimensional parameter space of the two detector design does not allow for this resource-intensive computation chain. However, it was shown in **??**, that the baseline resolution of the ionization channel roughly follows a linear law with the terms of the Maxwell capacitance matrix. Tempering this observation with further insights presented in the previous chapter **??**, the Maxwell and mutual capacitance terms can be used as a valid metric when discussing the influence of the design parameters on the detector resolution. The charge collection is broad expression covering the fiducial volume, the trapping rate and the signal generation by the drifting electric charges. While the real fiducial volume can only be accessed through experimentation, it can be inferred from the knowledge on the electric charge drifting in germanium (see paragraph **??**) and the theoretical fiducial volume obtained with electrostatic simulation (see paragraph **??**). A precise value for the electric charge trapping rate is difficult to forecast in the bulk. However, it is known that region of the crystal with low magnitude of electric field demonstrate a higher propensity to charge trapping. The next chapter **??** demonstrates using the analysis of the RED80 data, that over a critical threshold of $|\vec{E}| = 0.1\,\mathrm{V}\cdot\mathrm{cm}^{-1}$ (to be verified!!!), the trapping rate is constant. On further notice concerning the signal generation, the electric charge conservation equation **??** depends on the quality of the Faraday cage formed by the aluminium electrodes which is quantified by the total weighing potential (TWP) in paragraph **??**. A low TWP coupled with a high trapping rate could result in substantial fraction of the events to be discarded or worse, ill-reconstructed, in the analysis.

On those grounds, a metric is established for the study of the design parameters influence. For each scanned configuration, the variations over the terms of the Maxwell $\boldsymbol{C}$ and mutual $\boldsymbol{C}^m$ capacitance matrices, the fiducial volume fraction $\%_{fid}$, the electric field norm $|\vec{E}|$ as well as the weighting potentials Φ_X are documented. In some cases, the variation over the considered capacitance terms C_{XX} is more appropriately illustrated with a ratio:

$$\frac{C_{XX}\,(p = x)}{C_{XX}\,(p = p_0)} \tag{1.1}$$

where p is the scanned parameter, $p0$ a reference value (usually the default value) and x the scanned value. As the electric field norm $|\vec{E}|$ and the weighting potential Φ_X are scalar field and their variations are generally homogeneous in the crystal volume, it is challenging to propose a universal scalar quantity for discussion. Consequently, the illustration and features of these fields used for the scan interpretation are specific to the considered parameter and selected at the best of the authors' discretion.

For each detector designs, the configuration of the electrostatic simulation is set by several parameters. Thus, this study calls for a multi-dimensional scan over the design parameters and could even result in a semi-automated optimization of the design like what is achieved for the heat channel in chapter **??**. Nevertheless, the performance of the ionization channel cannot be gauged with a single quantity and invalidate such a ionization channel design optimization. As such, the study presented in this chapter focuses on understanding the influence of each parameter by carrying multiples one-dimensional. Only one parameter is scanned over at a time with all the other parameters sets to default values. Hence, the control quantities resulting from a scan can be compared to the default design value which was discussed in the previous chapter **??**. Although simpler, this method explicitly omits a massive portion of the parametric space. This introduces the risk of scanning far from an optimal configuration and collecting only marginal insights on the ionization channel design. However, this risk is heavily mitigated by the fact that the default configuration of the PL38 and the FID38 detectors designs presented in the chapter **??** are the product of a manual optimization inspired by the whole thesis work on ionization channel.

1.2 Common Parameters

1.2.1 Aluminium Thickness, h_{Al}

The thickness of the aluminium electrodes used in the COMSOL simulation is noted h_{Al}. It is not in itself a design parameter as the actual thickness depends on the fabrication process and is usually of about 50 nm. This value is much lower than any geometric feature in the COMSOL simulation which, if implemented as is, would induce a complex meshing and a long simulation time. As to keep the simulation resource cost reasonable, the electrostatics simulation are ran with a greater thickness than in reality at the expense of small supplementary errors. For the FID38 geometry, the electrostatic simulation is ran multiple times scanning over the electrode thickness h_{Al}. The table 1.1 presents for each value of h_{Al} the number of triangles in the mesh, the diagonal Maxwell capacitance of top collect (B) electrode C_{BB} and the relative error on this capacitance. The reference for the error calculation is considered to be the capacitance computed for the lowest value $h_{Al} = 0.1\,\mu\text{m}$.

As expected from simulating thin electrodes, the number of triangles composing the mesh is drastically increased. Also, as the electrodes presents a lower area, their capacitance is slightly lowered, eventually capping for the lowest thickness values. In other words, the computation of the capacitance term is getting more precise with decreasing electrode thickness. A trade-off

h_{Al}/µm	# Triangles	C_{BB}/pF	Relative Error / %
100	7413	20.419	7.3
30	13959	19.560	2.8
10	22504	19.232	1.1
3	34745	19.102	0.4
1	58815	19.053	0.1
0.3	76637	19.034	0.02
0.1	106057	19.029	0

TABLE 1.1: Scanning over the electrode thickness w_{Al} of the FID38 design. The control values are the number of triangles in the mesh, the first diagonal term of the Maxwell capacitance matrix and the relative error on the capacitance calculation with the lowest thickness $h_{Al} = 0.1\,\mu m$ chosen as reference.

is selected at $h_{Al} = 1\,\mu m$ with a relative error of 0.1 %. Indeed, this quantity is reminiscent of the relative error of 0.08 % induced by the chosen mesh scale "Fine" presented in paragraph **??**.

1.2.2 Chassis Distance, d_{Cu}

The chassis distance $d_{chassis}$ is the distance between the grounded copper chassis and the planar and lateral faces of the germanium crystal. Its default value is set to 3 mm for both the PL38 and the FID38 design. The scan is performed on a logarithmic scale from 0.1 mm to 10 mm. The results are presented in the figure 1.1 for the PL38 design and in the figure 1.2 for the FID38 design. Both figures display the terms of the Maxwell $\boldsymbol{C}$ and mutual capacitance matrix $\boldsymbol{C}^m$ along with the fiducial volume fraction $\%_{fid}$ as functions of the chassis distance $d_chassis$ for their respective detector design.

- Self-capacitance term decrease as the chassis distance increases. (more distance between the plate)
- Non-diagonal elements of the mutual matrix increases with the chassis distance
- As a result, the diagonal maxwell capcaitance decrease with the chassis distance.
- fiducial volume increases with chassis distance.
- PL38: fiducial volume increase explain by the shrinking of the exiting streamlines region.
- FID38: veto region depth decrease with the chassis distance, explaining the increasing fiducial volume
- 3mm is a good value. Trade-off with geometric constraint of the cryostat.

PL38
- the tWP decreases inside the crystal significanlty for <3mm. As the copper chassis is getting closer, more and more signal is induced on the electric ground. (plot twp in bulk ?)
- what about the enorm ?

FID38
- the enorm distribution is scaled down (slightly)
- twp increases with chassis distance, less signal is induced on the mass. (plot twp in bulk and veto region ?)

Also tru for the std of the twp, is it relevant ?

1.2.3 Bias Voltage, V_{bias}

The bias voltage V_{bias} corresponds to the voltage between the two main electrodes of the detectors. By default, it set to 2V.

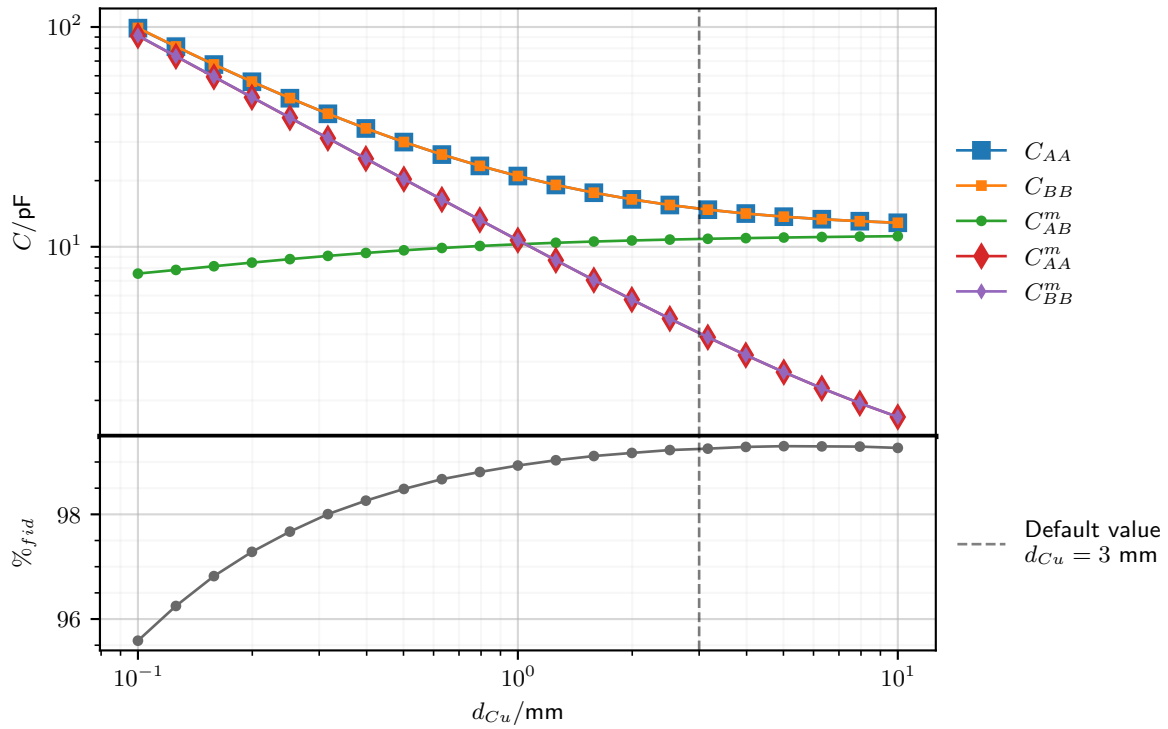

FIGURE 1.1: Maxwell and mutual capacitance terms and percentage of fiducial volume as a function of the chassis distance d_{Cu} for the PL38 design. The default value $d_{Cu} = 3\,\text{mm}$ is represented by the dashed vertical line. Error bars are smaller than the marker size.

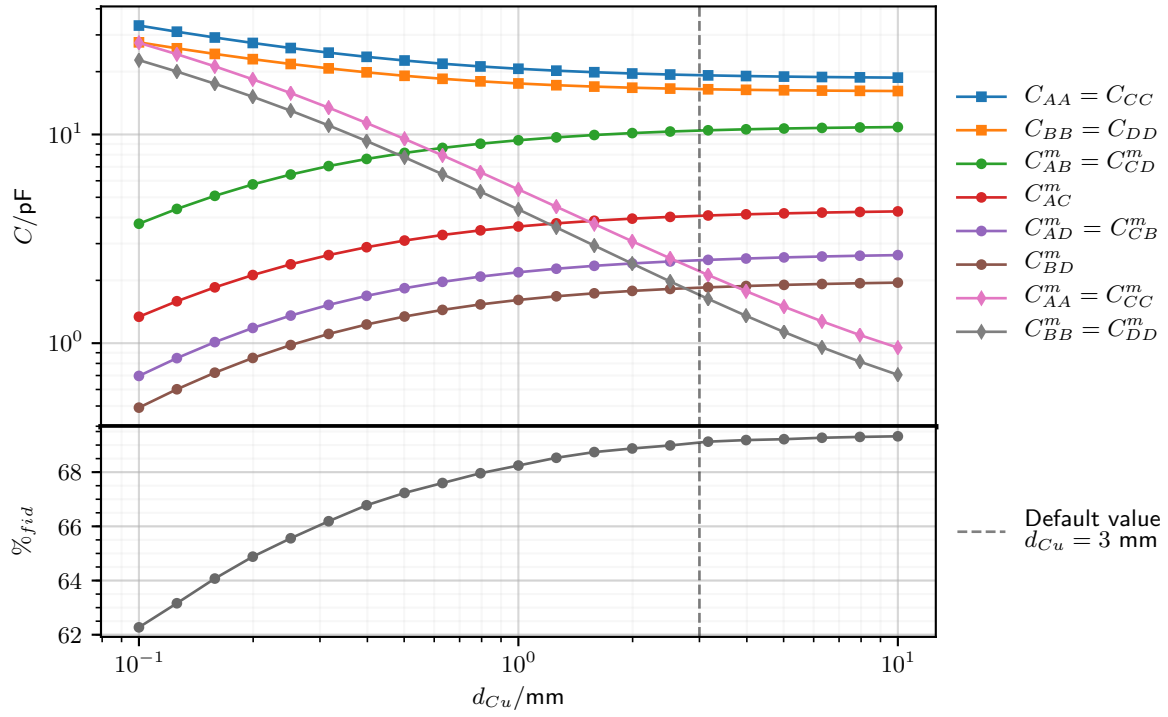

FIGURE 1.2: Maxwell and mutual capacitance terms and percentage of fiducial volume as a function of the chassis distance d_{Cu} for the FID38 design. The default value $d_{Cu} = 3\,\text{mm}$ is represented by the dashed vertical line. Error bars are smaller than the marker size.

- No change in capacitance, theoretical fiducial volume, twp.
- PL38 and FID38: enorm proportionnal to Vbias as expected. Low enorm region exacerbated at lowest Vbias values. (enorm curve ? danger fraction curve ?)

- Lowest Vbias possible is wanted, in order to benefit more from the double energy measurement with less Luke-Neganov effect. However, very high Vbias guarantees a direct trajectory for the electric charge and an execellent charge collection (see discussion in previous paragraph surely).

1.2.4 Polarization Symmetry, S_{bias}

The polarization symmetry S is a parameter used to set the individual polarization of each electrodes for the PL38 and FID38 (according to equation [eq?]).

- No change in capacitance and twp, independent from electrode polarization.
- PL38: enorm unaffected
- PL38: streamlines know very slight variation. For the asymmetrical polarization, more streamlines are exiting on the equatorial surface with an optimum for a symmetrycal polarization. (need fiducial plot!)
- note for PL38: mitigation of the symmetry thanks to lateral corner. Effect are exacerbated with a non-existent lateral corner (need confirmation and fiducial plot associated)
- FID38: asymmetrical polarization induces higher enorm fields in the vacuum surrounding the crystal.
- FID38: no cahnge for the enorm in the crystal, constant low enorm region and magnitude everywhere.
- FID38: negligible change on the streamlines near the equator

All in all: affecting the symmetry of the polarization theoretically seems to work. Nice to know:
- mitigate the effect of the NTD gluing affecting the local potential
- something else ? i dont think so

1.3 Specific to PL38

Presentation and scan over parameters specific to the PL38 detector.

1.3.1 Radius of the central hole for the NTD, r_{center}

The radius of the central hole r_{center} in the top electrode of the PL38 in order to glue the NTD in contact with the bare germanium crystal. By default, it is set to 1.5mm, in order to fit 2*2mm NTD. It could be extended to 3mm, in order to a big 4*4 NTD.

- the non-diagonal term is decreasing. Less area of the electrodes A, B facing.
- the self-capacitance capacitance of B slightly increases. With the hole in electrode A, the ground can face the electrode B from the top thus boosting ever so slighlty this capacitance term.
- in result, as the non diagonal term is dominant, still negligible deacreases in diagonal maxwell capacitance for A and B electrode.

- fiducial volume: slight(negligible) loss in theoretical fiducial volume fraction. In term of real fiducial volume, with this low e norm region with a bare germanium surface, we can expect

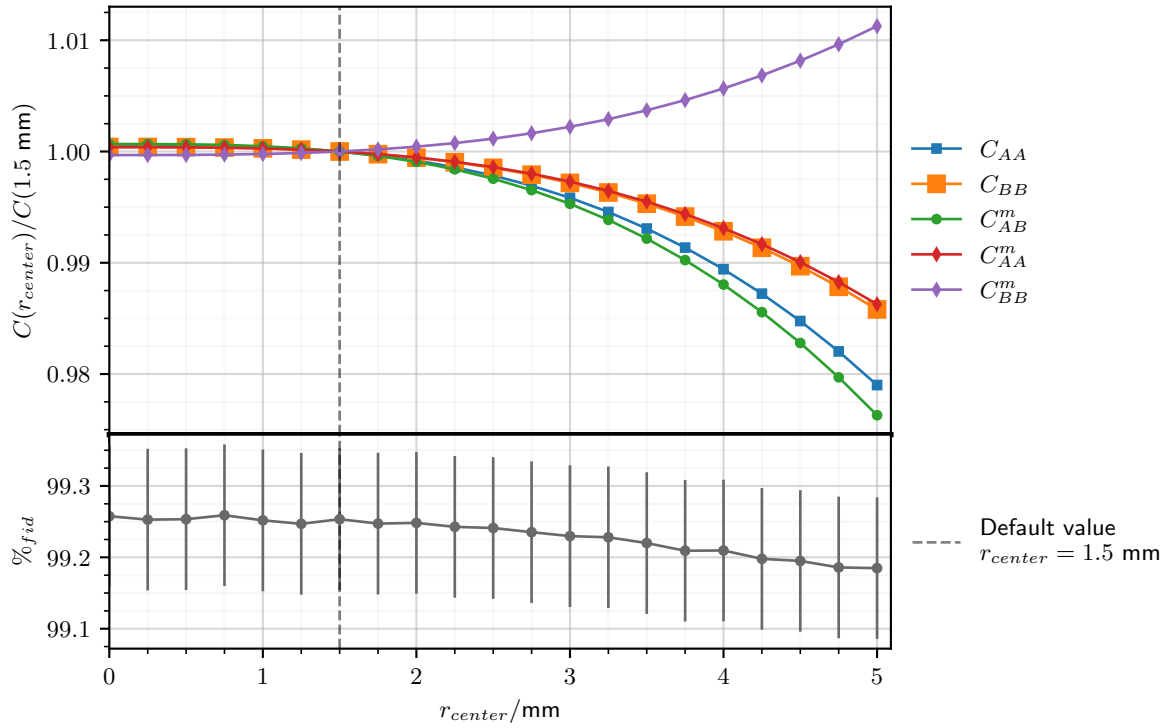

FIGURE 1.3: Maxwell and mutual capacitance tarms ratio and percentage of fiducial volume as a function of the radius r_{center} of the central hole of PL38 design. The capacitance term ratio is calculated with the default capacitance value as denominator. The default value $r_{center} = 1.5\,\mathrm{mm}$ is represented by the dashed vertical line. Error bars for the capacitance ratio are smaller than the marker size.

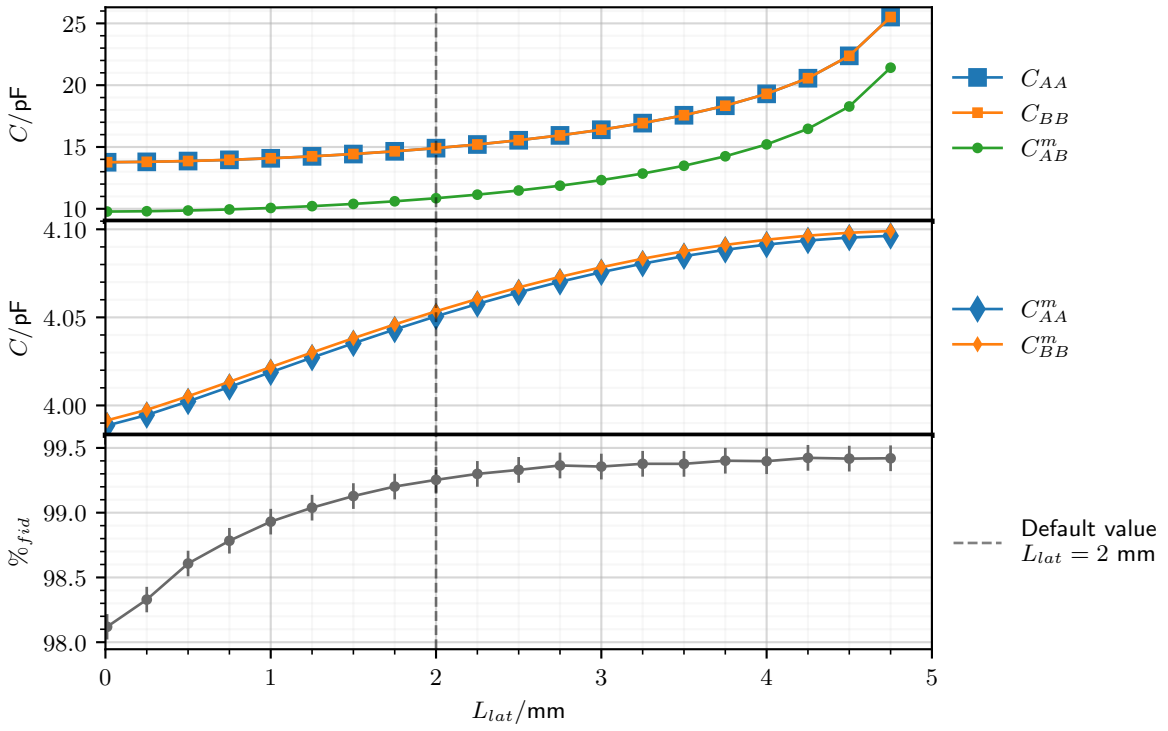

FIGURE 1.4: Maxwell and mutual capacitance terms and percentage of fiducial volume as a function of the corner length L_{lat} of the PL38 design. The default value $L_{lat} = 2\,\text{mm}$ is represented by the dashed vertical line. Error bars for the capacitance terms are smaller than the marker size.

recoil in this region to produce charges easily trapped on the surface, or with recombination problem.

- e norm |E|: with hole, creation of a low e norm region under the hole in the electrode. Streamlines are diverging from the hole/bare germanium and converging to the electrode (good for charge cllection)

- twp: a low TWP region appears under the hole. (from 1 to 0.97) so not so much moss, and on a small volume. (compared to the impact of the lateral corner).

Conclusion: it seems okay to do holes in the electrodes. Tradeoff , heat sensitivty at the cost of possible charge collection under the hole.

1.3.2 Corner length, L_{lat}

The corner length L_{lat} corresponds the height of the lateral face of the crystal covered by the planar electrodes. The default value is $2mm$.

- all mutual capacitance terms increase with the corner length. Explaining by the increase in electrode area facing each other and the ground. Self-capacitance is less affected, and start to cap further than 4 mm. The non-diagonal capacitance term is drastically increased, which can be explained by the electrode A and B getting closer with the increasing corner length. For large corenr length, the area of the electrode facing the crystal are facing almost entirely the oppsite electrode and can only perceive the electric ground through the tight bare equator. This could explain the capping in the self-capacitance of A and B.

- The fiducial volume fraction increases very slightly, almost reaching 100 %. Still, some streamlines are exiting the crystal at the equator and under the central NTD hole. - Streamlines are almost straight in the case of near-vanishing lateral corner, and bend alot with lateral corners.

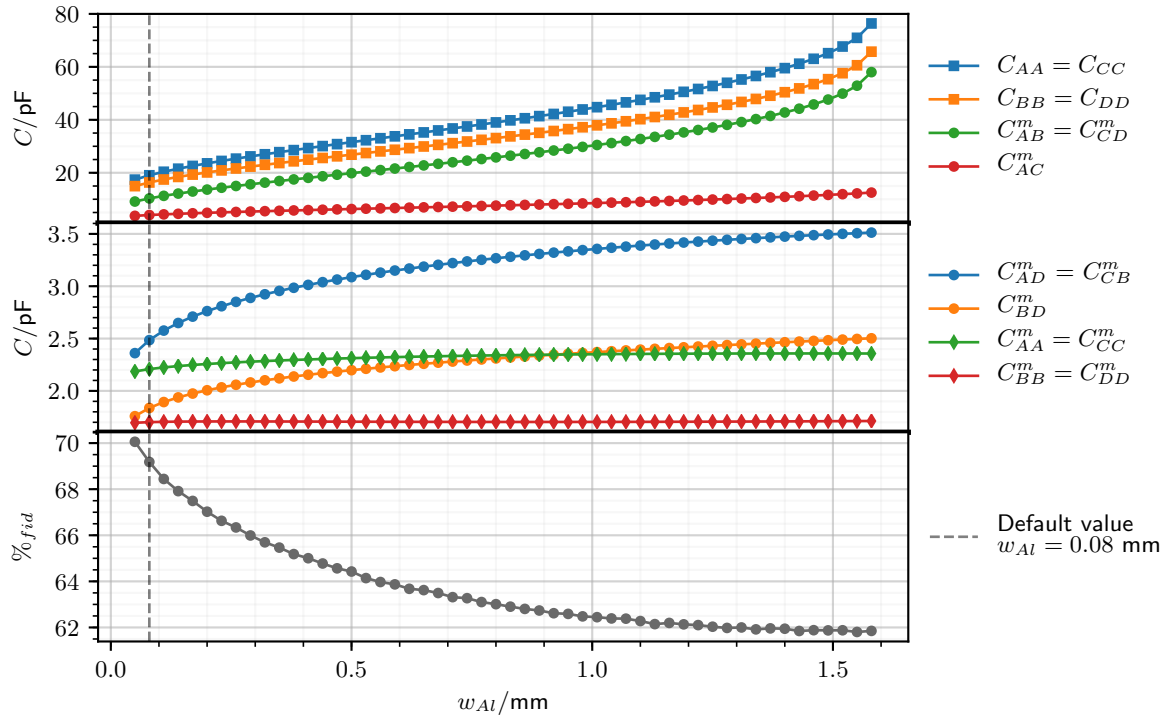

FIGURE 1.5: Maxwell and mutual capacitance terms and percentage of fiducial volume as a function of the width of the electrode rings w_{Al} of the FID38 design. The default value $w_{Al} = 0.08\,\text{mm}$ is represented by the dashed vertical line. Error bars are smaller than the marker size.

- e norm |E[: increasing e norm at equator as A,B electrodes are getting closer. In the corneres of the crystal, appearrance of growing low e norm region with slight divergence from the streamlines. Apparently not dangerous, because still a high enough enorm. (need confirmation) (danger fraction curve ?)

- TWP: is almost 1 in all the crystal for the full corner. Significant loss in TWP from the lateral face and deep into the crystal (lot of volume) with no corner. (average twp on surface curve ?)

Conclusion: - Balance between charge collection, stable signal generation VS capacitance terms, ionization channel resolution. Compromise selected to be $L_{lat} = 2\,\text{mm}$ with some room for adjustment if necessary.

1.4 Specific to FID38

Presentation and scan over parameters specific to the FID38 detector.

1.4.1 Width of the Electrode Rings, w_{Al}

The width w_{Al} of the rings composing the electrodes is set by default to $0.08mm$. It is subject to technical constraints as it is not possible to reliably aluminum electrode with a width inferior to $50\mu m$.

- fiducial streamlines: Significant decrease of the fiducial volume. Depth of the veto region is increasing with the ring width.

- capacitance: huge impact on all capcaitance terms.

- self-capcaitance is almost constant.

- the non-diagonal terms increase and seems to cap

- except for the coupling term between veto and colect on the same side, which increase drastically.
This is explained by an increase in the facing electrode area, and the veto and collect electrodes getting closer as the ring width rises.
- as this terem is dominant, the diagonal term of the maxwell matrix also increases drastically Capacitance increases significantly with the w_{Al}.

- enorm E: global increase of the enorm in the crystal (confirmed by the histograms) The low eneomr region under the veto electrodes seems to keep their size and amplitude, but go deeper into the crystal. Relevant with the gain in depth of the veto region. (mode enorm curve ?)

- twp: global increase of the TWP in the crystal + surface. This is confirmed by the TWP. At high ring width, the electric ground can also be perceived through the thin slit between electrodes, we understand that drifting electric charge have more difficulties to induce signal on the chassis. (mode twp curve ?)

Conclusion: Increasing the width of the ring is harmful for the fiducial volume and the ionisation resolution. Fiducial volume impact could be mitigated by twinking the Veto ratio. Possible to lower even more the capacitance by depositing even thinner electrode rings. Possible with future aluminium deposition techniques ? Only gain of having high electrode width would be the certainty that the electric charge are well collected on the electrode, and are not trapped very near the elctrode on the surface. This is unlikely as the electric field is gaining is strength as the charge is drifting near the electrode. Moreover, study on the electrode size by edelweiss ??

1.4.2 Central Pad Radius, r_{center}

The central pad radius r_{center} sets the size of the central pad for the top and bottom veto electrodes. It is set by default to $0.25mm$.

As r center increase, the planar space for the other planar electrode rings is lowered. This results in an increase in the planar ring density and a decrease in the planar ring interdistance d_{plan}.

- mild effect on capacitance.
- Only decreasing capacitance term are the self-capacitance of the main collect electrode B and D, as well as their coupling term C^m_{BD}. As the central veto pad grows, the innermost collect electrode rings are pushed away from the center. Apparently it emulates a loss in facing electrode area between B, D and the ground.
- the coupling between the two veto electrode is increased, which can be attributed to the growth of the central veto pad facing eachother.
- highest increase is for the coupling term between same side veto and collect electrode. Indeed, this is a direct effect of the lowered interdistance between the electrode.
- As these term are dominant, the diagonal maxwell capacitance do increase with the central pad radius.

- fiducial streamlines: loss in fiducial volume under the veto.
the loss is centered into the crystal and should not represent that much fiducial volume fraction. Negligble for a 2*2mm NTd size for $r_{center} = 1.5\,\text{mm}$. the effect is more noticeable for higher value.

- e norm |E|: for allr_{center}, there is a low enorm region under the central veto electrode. when r_{center} increases, the low enorm region is getiing bigger and gets deeper into the crystal. Merging of the top and bottom low enorm regions at 3mm, there is an inversion of the electric field direction under the central veto electrodes. (illustration ? no illustration ?)

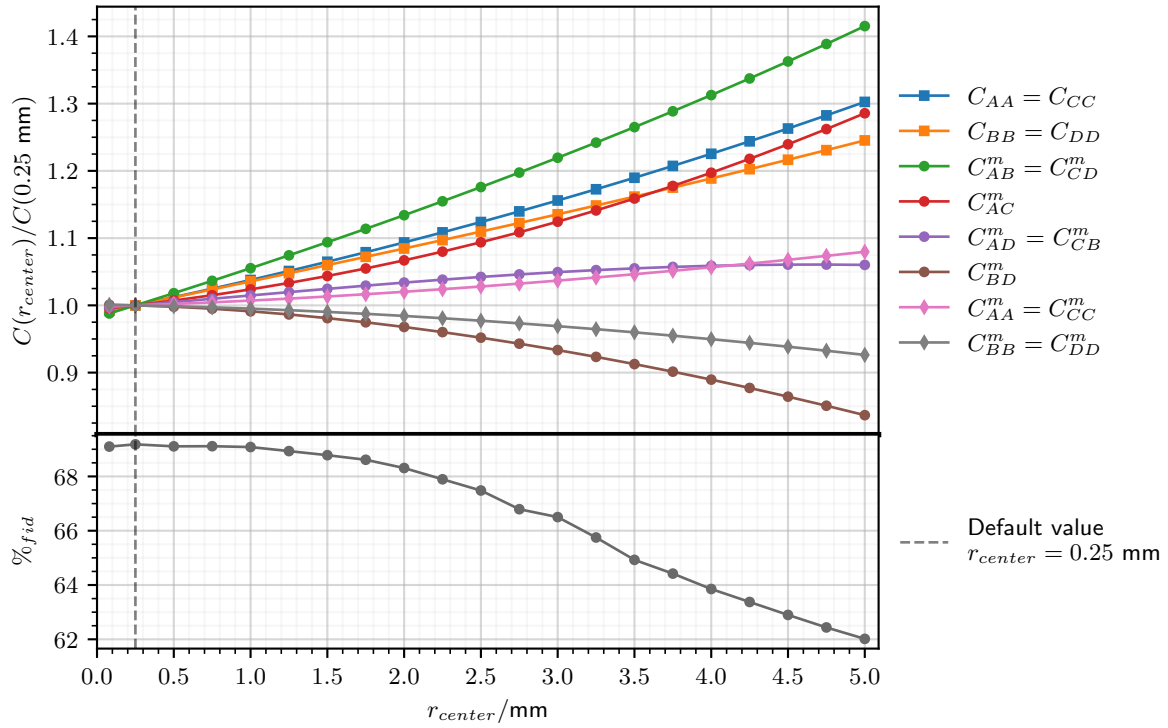

FIGURE 1.6: Maxwell and mutual capacitance terms and percentage of fiducial volume as a function of the width of the radius of the central pad r_{center} of the FID38. The default value $r_{center} = 0.25\,\mathrm{mm}$ is represented by the dashed vertical line. Error bars for the capacitance ratio are smaller than the marker size.

- twp: having a high r_{center} boosts the twp in the crystal (center) as there is more veto electrode area, there is more signal induced on it, and less signal induced on the ground. (illustration ? twp under the veto electrode ? or just numbers)

Conclusion:
- high r center in the case of NTD gluing on veto electrode. Not favored for now.
- Loss in fiducial volume and higher capacitance. Definitely we want the r_{center} to be as low as possible.
- however, with the lowest $r_{center} = 0.08\,\text{mm}$, the depth of the veto region under the central pad is too shallow, and fiducial streamlines come very close the the surface. So $r_{center} = 0.25\,\text{mm}$ is a good balance.

1.4.3 Edge Veto Electrodes

The rings of the veto electrodes near the planar edge of the crystal are called the edge veto electrodes. Due their important role in shaping the electric field in the corners of the crystal and the constraints on the aluminum deposition at this location, the shape of these corner veto electrodes could be of importance. The constraints on the aluminum deposition depends on the techniques used. When using a deposition with mask, aluminum cannot be closer than 0.3mm from the edge of the crystal. This would results in the creation of a bare edge of width $w_{edge,bare} > 0.3mm$. In the case of a deposition on the whole planar faces followed by photolithography, aluminum cannot be removed closer than 1mm from the edge of the crystal. This technique thus results in wide corner veto electrodes of width $w_{outer} > 1mm$. By default, the electrodes of the FID38 are deposited with mask and the corner veto electrodes are closest to the edge with $w_{edge,bare} = 0.3mm$ and a minimal width of $w_{outer} = 0.08mm$.

Width of Bare Germanium Edge, w_{bare} Width of Outer Veto Electrode Ring, w_{outer}

Thin Outer Ring Spaced from the Crystal Edge, Scan over w_{bare}

As the width of the bare edge increases, the free space available for the deposition of the other planar electrode ring diminishes. As a result, with the parameter w_{bare} rising, the planar ring spacing d_{plan} decreases.

- capacitance: high dead edge induces an increase in capacitance, due too the lowered planar spacing.
- lot of different behaviors ! But only light variation documented, in the range of 5 %.
- coupling term same side veto collect C^m_{AB}: decreases for low or high value of w_{bare} with a maximum near 0.6 mm. for low w_{bare} value, the planar spacing is high which explain the lowered capacitance between same side veto and collect electrode. For high w_{bare}, the planar spacing is diminished, explaining the maximum, but is eventually dominated by the large spacing between the planar rings and the lateral rings.
- coupling term veto C^m_{AC}: increases with w_{bare}
- coupling term collect C^m_{BD}: decreases with w_{bare}
- self-capacitance of the veto C^m_{AA}: maximum with $w_{bare} = 0.3\,\text{mm}$
- self-capacitance of the collect C^m_{BB}: minimum with $w_{bare} = 0.4\,\text{mm}$
- diagonal terms of the Maxwell matrix: follows the dominant term C^m_{AB}, with maximum spread between 0.3 mm and 0.8 mm.

- fiducial streamlines/fraction: change slightly the shape of the fiducial volume. Slight decreases in fiducial volume, percent - streamlines: at corners, the veto streamlines are changes, increasing the veto region at he corner. Also creates a corner region mentioned on scheme **??** where the streamlines exiting the crystal.

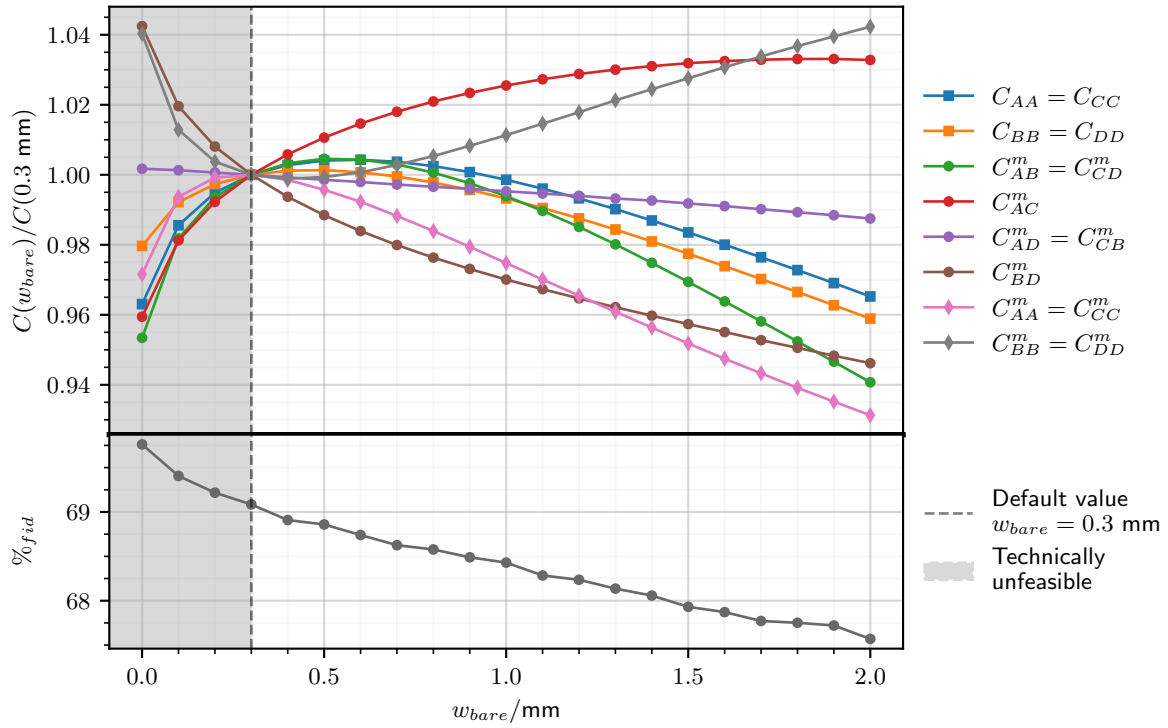

FIGURE 1.7: Maxwell and mutual capacitance terms ratio and percentage of fiducial volume as a function of the width of the bare edge w_{bare} on the planar edge of the FID38 design. The capacitance term ratio is calculated with the default capacitance value as denominator. The default value $w_{bare} = 0.3\,\mathrm{mm}$ is represented by the dashed vertical line. A width strictly inferior to 0.3 mm is technically unfeasible which is represented by the shaded area. Error bars are smaller than the marker size.

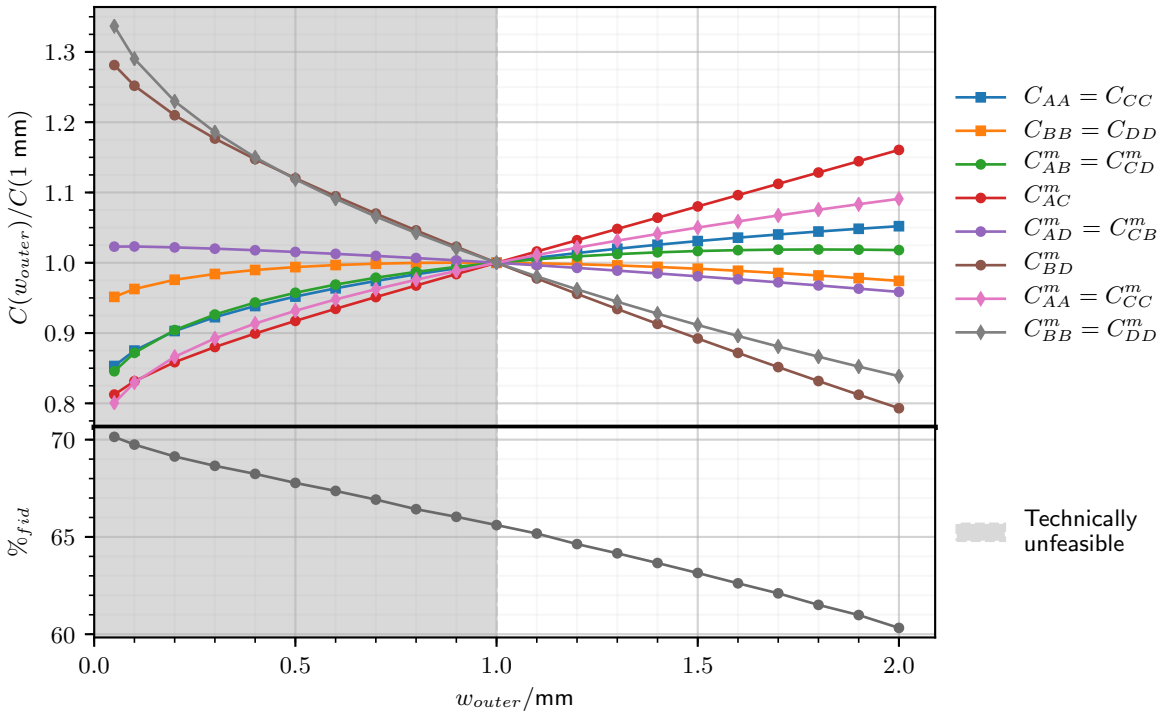

FIGURE 1.8: Maxwell and mutual capacitance terms and percentage of fiducial volume as a function of the width of the outermost veto ring w_{outer} of the FID38 design. The capacitance term ratio is calculated with the capacitance value at $w_{outer} = 1\,\text{mm}$ as denominator. A width strictly inferior to 1 mm is technically unfeasible which is represented by the shaded area. Error bars are smaller than the marker size.

(zoom on the streamlines on corner ?) (analytical curve possible, by considering the danger region to have a triangle profile)

- e norm |E|: affects slightly the position of all the electrodes and also the position of the low enorm region under the veto electrodes. (Might affect the shape of the enorm hist slightly) Also, it seems that the very corner possesses a low enorm. This makes corners a dangerous, uncertain place for charge collection.

- twp: corners of their twp slightly decreased under the "normal" twp for veto region. how dangerous is it for the surface trapped event in the danger corners ?

- Conclusion: Best solution would be a $w_{bare} = 0\,\text{mm}$ which is not currently feasible. A high w_{bare} would reduce marginally the capacitance values at the cost of creating large corner regions with uncontrolled charge collection. All in all, the minimum technically feasible value $w_{bare} = 0.3\,\text{mm}$ seems to be the best configuration for a thin outer veto electrode ring.

Large Outer Ring on the Crystal Edge, Scan over w_{outer}

As the width of the outer ring w_{outer} increases, the free space available for the deposition of the other planar electrode ring diminishes. As a result, with the parameter w_{outer} rising, the planar ring spacing d_{plan} decreases.

-capacitance

- dominant term: C^m_{AC} increases and reach a maximum near 1.5 mm.

- the collect coupling term C^m_{BD} decreases significantly. Collect electrode are more and more "facing" the growing outer veto electrode which overshadow the influence of the opposite collecting electrode

- also, the self-capacitance of the collect electrode decreases. With a rising w_{outer}, there is less free planar space for the deposition of the planar rings, which emulates a decreases in the collect electrode B,D facing the ground.
- diagonal veto term of the Maxwell matrix: increase and cap, following the trend of C^m_{AC}
- diagonal collect term of the Maxwell matrix: pretty constant with a maximum at the default value 1 mm. The increasing trends of the veto collect coupling term C^m_{AB} is mitigated by the trends of the other capacitance relative to the collect electrodes.

- fiducial volume: decreases with w_{outer}, because the veto region on the corners are getting bigger. As this gain in veto volume is located on the periphery of the crystal, it represents a significant decreases in volume.

- enorm: low enorm below the outer veto electrode ring gets deeper and closer to the center. In agreement with the growth the corner veto region. - the bulk and surface region see their enorm level decrease (enorm distribution mode curve ?)

- twp: as w_{outer} rises, the twp is dramatically improved in the corners and it also raises the twp in the whole crystal (few percent) (bulk twp, and corner twp curves ?)

- Conclusion: the influence on the capacitance term is noticeable but not that significant. On the other hand, the fiducial volume is significantly impacted bu the parameter w_{outer}. The best design solution would be to have a minimal width of $w_{outer} = 0$ mm which is not technically feasible. Thus, for now, the best configuration would be to consider the lowest possible width of 1 mm

Comparing the Two Geometries

- Comparing thin electrode and large electrode: Both studies points towards the same best solution: a thin outer veto electrode ring on the edge of the crystal for low capacitance values and higher fiducial volume. A configuration which is not possible technically for now. Now, comparing the best compromise offered by the two topologies: (table with capacitance values and fiducial volume, and other bonus category: danger zone volume !)

Conclusion: thin electrode favored for now, but backup design is with large electrode for now. Waiting for experimentations with danger corner region to have more insights on the danger corner region.

1.4.4 Equatorial Distance, d_{eq}

The equatorial distance $d_{equator}$ corresponds to the distance between the two veto electrodes on the middle of the lateral surface of the crystal. By default, it is set to 1 mm.

- capacitance: significant rise for 0.1mm when the two veto electrodes are close to each other. slight increase for high distances as the lateral electrode are getting closer.
- for low equatorial distance, veto coupling term increase as expected.
- the coupling between same side veto and collect increase with equatorial distance due to the decrease in the lateral spacing.
- the two trends mitigates for the diagonal Maxwell capacitance of the veto which shows a very spread minimum between 2 mm to 5 mm.
- the diagonal term for the collect electrode is slightly increasing.

- fiducial streamlines/fraction: strictly lower than 2.8 mm: existence of equatorial streamlines from 2.8 mm, the equatorial streamlines vanish and the bulk streamlines come on the lateral surface of the crystal. This will generate surface trapping, and nullify the use of the FID design aiming at discarding any surface event. According to the fiducial graph, the fiducial

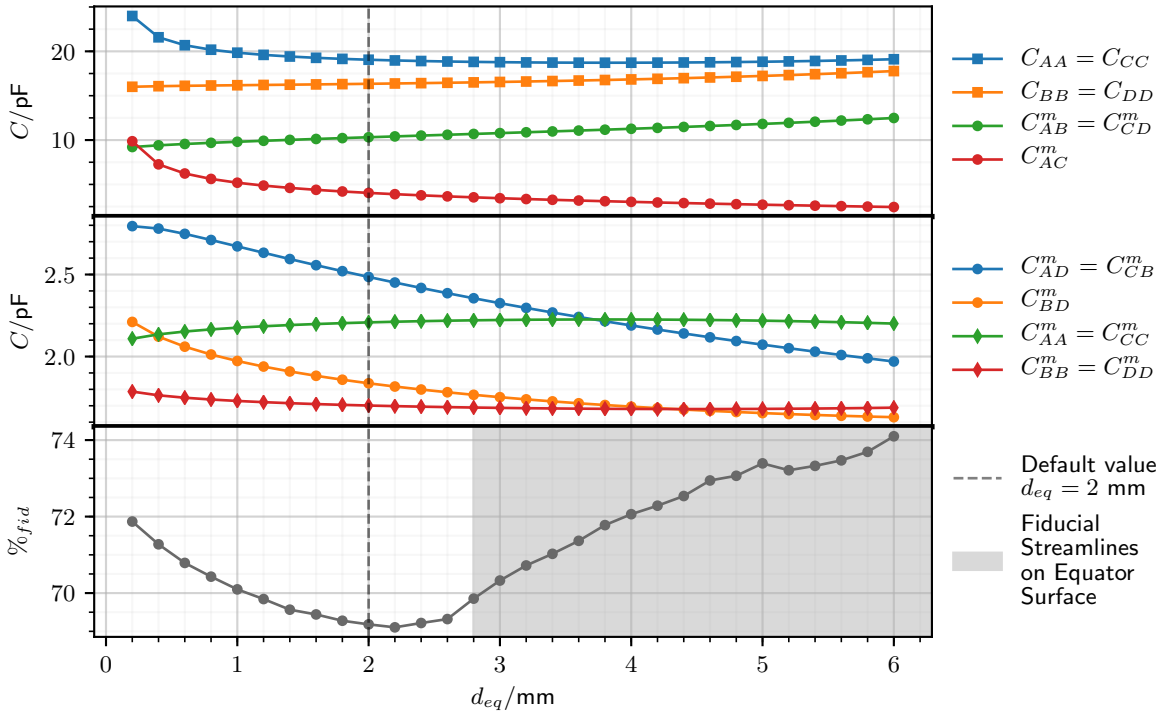

FIGURE 1.9: Maxwell and mutual capacitance terms and percentage of fiducial volume as a function of the equatorial distance d_{eq} of the FID38 design. The default value $d_{eq} = 2$ mm is represented by the dashed vertical line. Starting from 2.8 mm, fiducial streamlines are on contact and exiting the crystal on the equatorial surface, this is represented by the shaded area. Error bars for the capacitance ratio are smaller than the marker size.

fraction gets an minimum for 2.2 mm. Indeed, at low d_{eq} values, the fiducial volume fraction is increasing because the veto regions on the surface loses in depth and so in volume.

- e norm |E|: for small equatorial distance: high enorm region and very small low enorm shadow on equator for increasingly high equatorial distance: the low enorm region is growing significantly and eventually covers the majority of the lateral surface.

- enorm hist: there is a uniformisation of the efield norm in the crystal as the distance is getting bigger. Uniformization towards main peak. (enorm distribution std and mode curve ?)

- twp : significant loss at high equator distance, comming from the surface (same observation as corner lenght for PL38) According to twp hist, optimum at 2mm ? (Confirmation needed, twp median and std curves)

Conclusion: Balance on the capacitance with a middle equatorial distance in order to keep the capacitance low. Fiducial volume optimization points towards a small equatorial distance. Good balance on a spread range from 1.2 mm to 2.6 mm $d_{eq} = 2$ mm. There should be a huge correlation with the interdistance of the elctrodes and the Veto ratio for polarization. Mitigation of the fiducial streamlines behavior with the Veto Ratio, maybe. Maybe, 1mm appears to be the optimum for the default parameters used for FID38, and there may be another optimal values for different parameters.

1.4.5 Polarization Ratio, R_{veto}

The polarization ratio R_{veto} is one of the parameters fixing the polarization of each electrode of the FID38 according to equation [eq?]. By default, it is set to 0.25.

As the polarization ratio R_{veto} only sets the electric potential of the electrodes and does not affect their geometry, the capacitance matrices as well as the weighting potentials remain unaffected for this study.

- fiducial streamlines, (need for the curve !) (need a figure presenting the streamlines for the FID38 in planar polarization) The fiducial volume fraction decreases with R_{veto} and reaches a maximum of about 95 %for $R_{veto} = -1$. This configuration (not the only value when this happens, for other ratio too) corresponds to an electric field very similar to a planar detector (like the PL38 design) where same-sided electrodes are equally collecting drifting charges. This mode of operation (discussed previously in chapter **??**, paragraph?) is not compatible with the tagging of the surface events. The fiducial volume fraction reaches a minimum for $R_{veto} = 1$ when $V_A = V_D = -V_B = -V_C$. In this configuration, the electric field in the bulk of the crystal is nullified, if not slightly reverses (due to the higher total number of veto electrode rings, need confirmation). For $R_{veto} \leq -0.3$, the FID38 detector is in a planar-like polarization. There are no veto region. All the electrodes behaves as collecting electrodes. For $R_{veto} \geq -0.3$, shallow veto regions appears. Small region of low electric field norm are presents under the veto electrodes rings. However, the electric field in the equatorial region has the same direction as the electric field in the bulk region. For $R_{veto} \geq 0$, veto regions along with the low $|\vec{E}|$ regions associated are getting deeper. The equatorial volume has vanished as the fiducial streamlines are now touching the crystal equatorial surface. For $R_{veto} \leq 0.2$, the equatorial volume is present with an electric field of opposite direction to the one in the bulk region. The electric field structure is standard for a FID operation as presented in the scheme **??**. As the polarization ratio R_{veto} increases, the veto regions and the equatorial region grow in size, reducing the fiducial volume. Eventually, the regions of low electric field magnitude under the veto electrodes are big and deep enough to merge and hold the bulk of the crystal.

- The magnitude of the electric field in the bulk of the crystal decreases with the rising R_{veto}. Far from the electrodes, the interleaved same-sided veto and collect electrode rings appears have the influence of an equivalent planar electrode of electric potential $V = \frac{V_B+V_A}{2}$ and so the perceived electric field norm in the bulk is $E = \frac{V_B+V_A-V_D-V_C}{2H_{Ge}} = ...$ (this calculation should

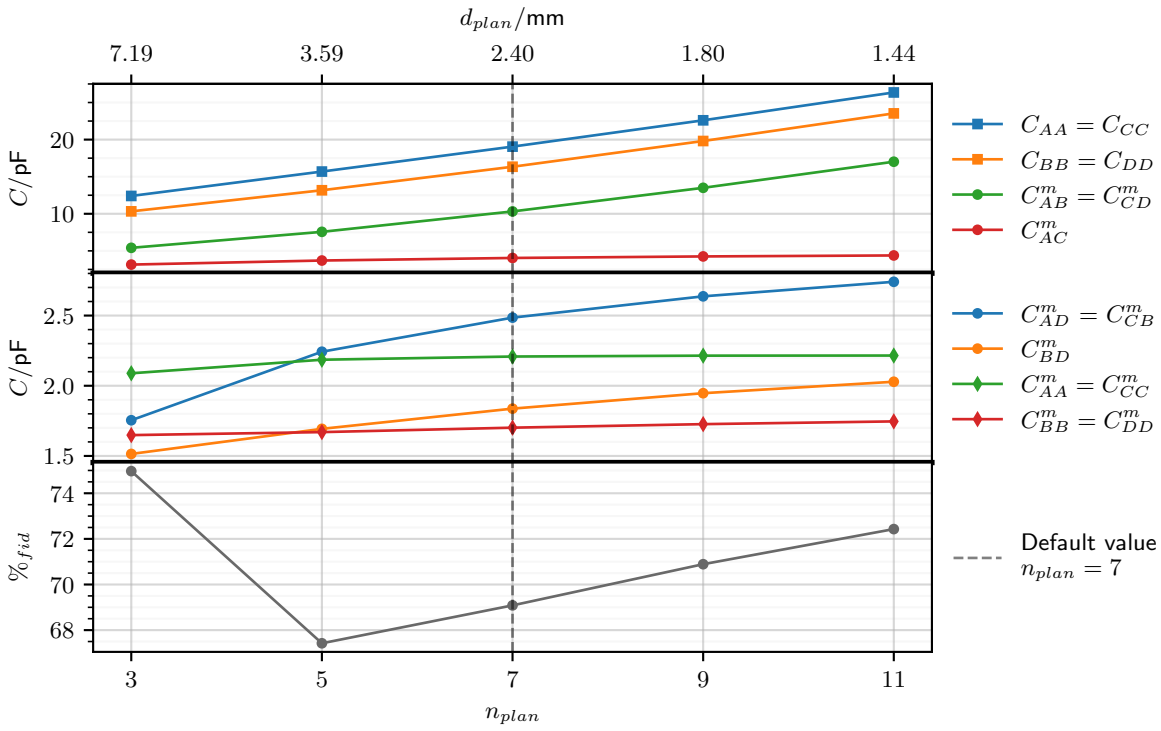

FIGURE 1.10: Maxwell and mutual capacitance terms and percentage of fiducial volume as a function of the width of the number of planar electrode rings n_{plan} of the FID38 design. The default value $n_{plan} = 7$ is represented by the dashed vertical line. The parameter n_{plan} is restricted to odd integers in order to assign the central pad and the outermost rings to the veto electrodes A and C. Error bars are smaller than the marker size.

appears when introducing the norm of the electric field and discussing the figure at default value. The calculation explain the phenomenon observed now during the scan over R_{veto}).

- Conclusion: R_{veto} should be high enough to be in a polarization mode compatible with the tagging of surface events, while being low enough to keep a good fiducial volume fraction. The lower threshold on a valid R_{veto} is apparently imposed by the existence of an equatorial region with an electric field of opposite direction to the bulk electric field. Is it really necessary to have opposite direction ? Yes, or else, a lot of bulk events would deposit some signal on the equatorial rings. So, we have a hard constraint of $R_{veto} > 0$. In order to have the actual existence of the equatorial region, the influence of the veto equatorial rings should be greater than the collect ring, that is to say, fiducial streamlines should not contact with the equatorial surface. the obvious solution is to increases the polarization ratio R_{veto} at the detriment of the fiducial volume. It might also be possible to tweak the equatorial distance d_{eq} to mitigate the low electric potential of the veto electrode.

1.4.6 Number of Planar Electrode Rings, n_{plan}

The number n_{plan} of rings on a planar surface composing the main collect and veto electrodes. As the FID38 design is based on the interleaved topology, it is necessary to assign the central aluminium pad and the outermost ring to the veto electrodes (justification, explanation for that ?). Therefore, n_{plan} is an odd integer. As the electrode rings are evenly spread on the fixed free planar surface, their number sets the ring spacing and their density on the surface. By default, n_{plan} is set to 7 which corresponds to a spacing of the planar ring is $d_{plan} = 2.40\,\text{mm}$.

All the capacitance term follow the same trend: they increase with the increasing number of planar ring. A higher number of aluminium rings emulates a higher area of facing electrodes in the parallel-plates capacitance equation **??**. As a result, capacitive couplings between all electrodes as well as the ground are greater.

Apart from the first point, the fiducial volume grows with an increasing number of planar rings. This is explained by a loss of depth and volume of the surface veto region. This is consistent with the study of the electric field magnitude. With few planar electrodes, there are large diffuse region of low electric field magnitude deep into the crystal. With a high number of planar electrodes, the low magnitude regions are smaller and near the surface bellow the veto electrode rings. The magnitude of the electric field is more uniform in the crystal.

The minimal number of planar electrodes $n_{plan} = 3$ is particular. For this configuration, the fiducial volume is maximal (should I show an image of the streamlines ?). However, a lot of fiducial streamlines are almost parallel to the planar surface, which could be problematic with the transversal trajectory of the electrons. Moreover, the regions of low magnitude comes into contact with the planar surface, surely resulting in high fraction of trapped event on the planar surface. Indeed, a dangerously high fraction of the volume has a very low electric field. (need danger fraction curve!).

A low number of planar ring results in a significant loss of the total weighting potential level near the center ($r \lesssim 10\,\text{mm}$) of the crystal, while the outer region of the crystal remains under the influence of the fixed number of lateral electrode rings. (need table with value of twp near center for different n_{plan} values!)

The number of planar electrode rings n_{plan} can be used to have a better control on the shape of the electric field with a higher fiducial volume at the expense of a significant increase in capacitance. Alone, this parameter mainly affect the behavior near the center of the detector as the number of lateral electrode ring n_{lat} is fixed. Its effect on the fiducial volume is strongly correlated with the influence of the polarization ratio r_{veto}. In the later paragraph 1.4.8, the number of planar ring n_{plan} is scanned over with adapted number of lateral electrode n_{lat} and the polarization ratio R_{veto}.

1.4.7 Number of Lateral Electrode Rings, n_{lat}

The number n_{lat} of rings on the lateral surface composing a main collect and veto electrodes (either the top collect and top veto or the bottom collect and bottom veto). In order to keep the interleaved topology of the FID38, the center-most lateral aluminium ring is assigned to a veto electrode while the ring closest to the crystal corner is assigned to a collect electrode. As a result, the parameter n_{lat} is an even integer. Similarly to the number of planar electrode rings n_{plan} described in the previous section 1.4.6, the number of lateral rings sets the spacing between the lateral rings as the electrode rings are spread evenly on the free lateral space of fixed height. By default, n_{lat} is set to 2 which converts to the lateral spacing $d_{lat} = 1.98\,\text{mm}$.

The observations resulting from the scan over n_{lat} are very similar to the ones from the scan over the number of planar rings n_{plan} presented in the previous paragraph 1.4.6, with a few differences. With an increasing number of lateral rings, almost all the capacitance terms increase and the fiducial volume grows. Moreover, the total weighting potential ins the surface region gets slightly higher with a higher number of lateral right. (table needed?)

For this scan, the increasing fiducial volume is associated to the shrinking of the surface veto regions, the parameter n_{lat} does not affect much the center ($r \lesssim 10\,\text{mm}$) of the crystal. However, this growth is also associated to the disappearance of the equatorial volume. Indeed, for $n_{lat} \leq 4$, fiducial streamlines comes into contact with the equatorial surface and leave the crystal. These configurations would results in a lot of surface trapping at the equator and would not be able to tag the surface events near the equator.

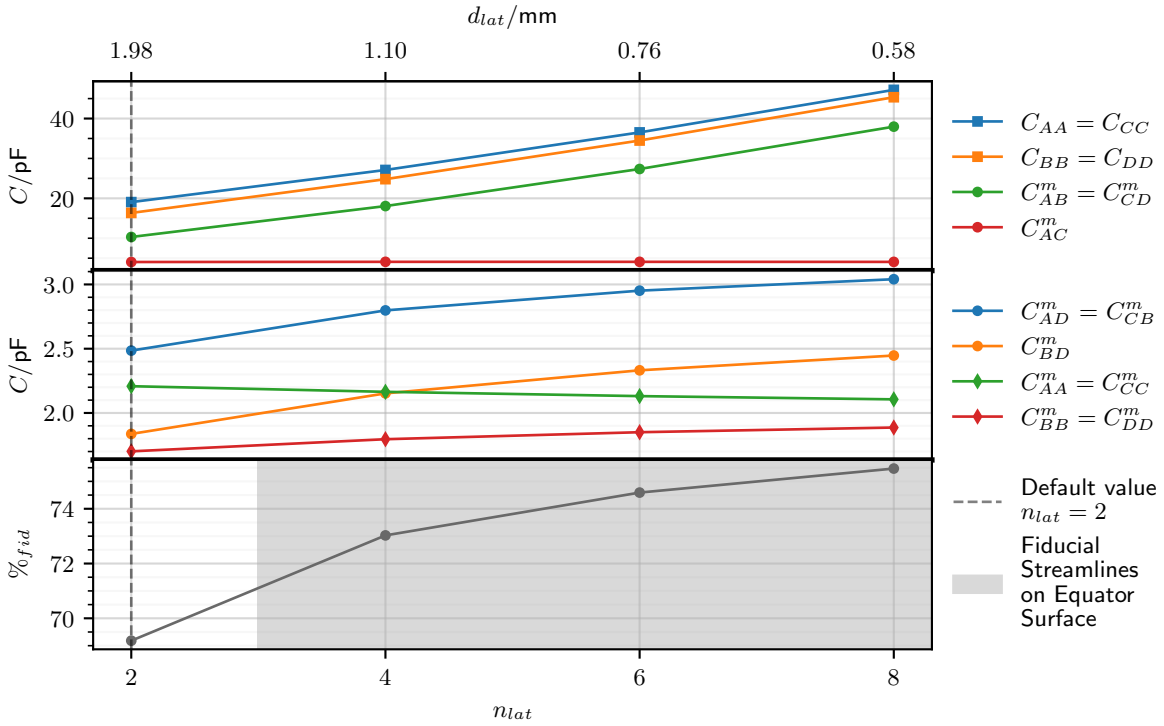

FIGURE 1.11: Maxwell and mutual capacitance terms and percentage of fiducial volume as a function of the width of the number of lateral electrode rings n_{lat} of the FID38 design. The default value $n_{lat} = 2$ is represented by the dashed vertical line. The parameter n_{lat} is restricted to even integers in order to assign the centermost equatorial rings to the veto electrodes A and C. Error bars are smaller than the marker size.

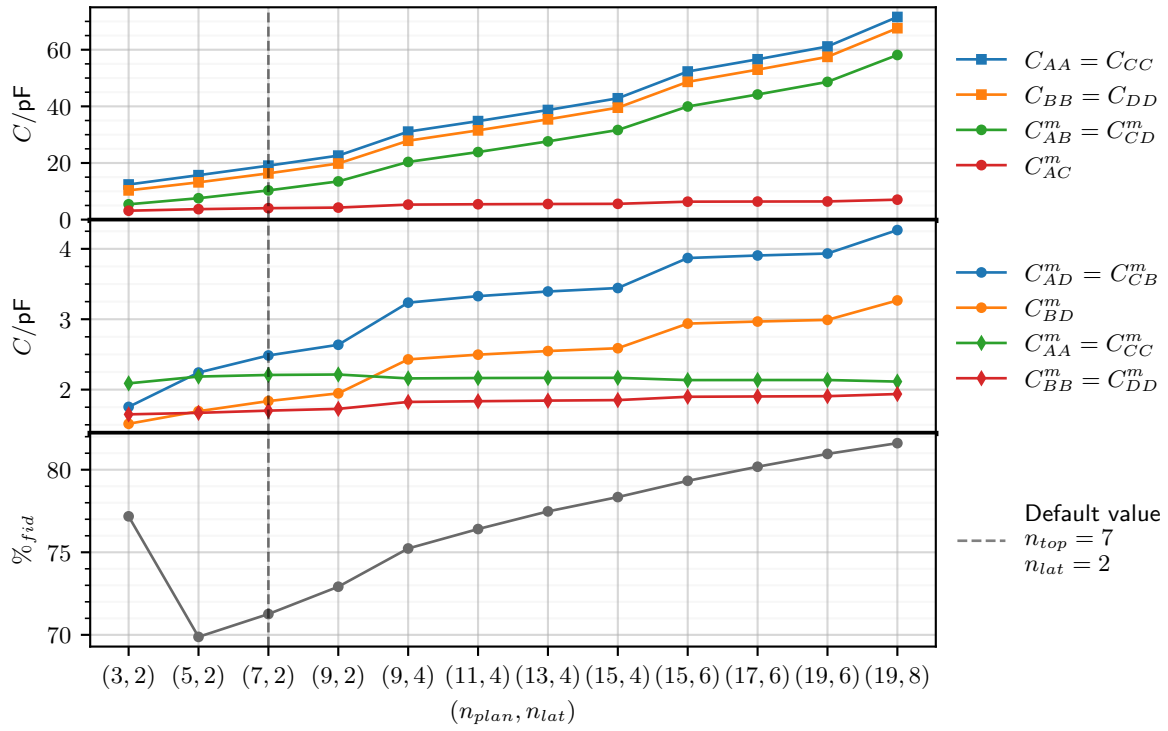

FIGURE 1.12: Maxwell and mutual capacitance terms and percentage of fiducial volume as a function of the number of planar and lateral electrode rings (n_{plan}, n_{lat}) with adapting equatorial distance d_{eq} and polarization ratio R_{veto}. The default configuration $(n_{plan}, n_{lat}) = (7, 2)$ is represented by the dashed vertical line. Error bars are smaller than the marker size.

1.4.8 Global Density of the Electrode Rings

Scan over multiples parameters: R_{veto}, d_{eq}, n_{plan}, n_{lat}.

The equatorial distance is set to be equal to the lateral electrode spacing:

$$d_{eq} = \frac{H_{Ge}}{1 + 2n_{lat}} \approx d_{lat} \tag{1.2}$$

The polarization ratio depends on the equatorial distance and the number of lateral electrode. It is adapted by checking the existence of an equatorial region of satisfying size and with an electric field of opposite direction to the bulk electric field. An empirically found function is used to set polarization ratio:

$$R_{veto} = \left(1 + 4\frac{d_{lat}}{d_{eq}}\right)^{-1} \tag{1.3}$$